Film Cooling from Two Staggered Holes Rows of Opposite Injection Angles with Downstream Row Embedded in Arc Trench

Dr. Assim H Yousif
Machines & Equipments Engineering Department, University of Technology/ Baghdad
Email:uot_magaz@yahoo.com
Humam Kareem Jalghaf

Revised on: 21/1/2013 & Accepted on: 4/7/2013

Abstract

Experimental investigation of film cooling from two staggered rows holes, backward and forward; of opposite injection angles has been done. The forward holes row was embedded in arc trench. The aim of using arc trench is to enhance the poor mechanical properties of that in rectangular trench. The results of film cooling performance are given here in a form of adiabatic cooling film effectiveness and heat transfer coefficients. In the tests test warm air is blown through tunnel, and cold air through the plenum chamber. When the warm air flowed through the test section it heated the model downstream. Infrared camera is used to measure the model surface temperatures. The comparison with the same holes arrangements and same holes and trench dimensions between existing rectangular trench results and present arc trenched showed that the film cooling thermal performance for both cases are approximately very close with slight differences, these differences are more or less according to the values of blowing ratios.

Keyword: film cooling**,** injection angles, arc trench, effectiveness, blowing ratio.

التبريدالغشائي الناجم من صفي ثقوب متعرجة ذات فتحات نفث متعاكسة مع وضع الصف السفلي في شق قوسي

الخلاصه:

لقد اجري اختبار عملي لغشاء التبريد من صفي فتحات متخالفة ذاتزوايا نفث متعاكسة امامية وخلفية. الصف الخلفي وضع في شق قوسي. كان الهدف من استخدام الشق القوسيكبديل للشق المستطيل هو لتحسين الخواص الميكانيكيه الفقيره للشق المستطيل .النتائج التحليلية لأداء غشاء التبريد تقدم هنا بدلالةالفعالية الادياباتية لغشاء التبريد ومعامل انتقال الحرارة.في التجارب العملية ينفخ هواء دافئ داخل مجرى مصصم لهذا الغرض والهواء البارد من خلال غرفة الجلسة. عند تدفق الهواء الدافئ خلال مقطع الاختبارفأنه يقوم بتسخين نموذج الاختبارالموجود في مقطع الفحص. تم استخدام كاميرا الأشعة تحت الحمراءلقياس درجاتالحرارة لسطح النموذج اسفل صف الاختبار.

أظهرت نتائج الدراسة الحالية أنه لنفس ترتيب الثقوب والابعاد الهندسية للشقوقعند المقارنة بين الشق المستطيل الموجودة نتائجه اصلا في المصادر والشق القوسي الحالي أنالأداء الحراري لغشاء التبريد في كلتا الحالتين يكون متقارب جدا مع وجود اختلافات طفيفة تتغير وفقا لقيم نسب النفخ.

INTRODUCTION:

Gas turbines are being considered to become the first choice for future power generation systems , because of their high fuel conversion efficiency and reduced power generation cost. In recent years various studies of gas cycle based power plants have shown that increasing turbine inlet temperature can substantially improve the overall power plant efficiency [1]. And high values of turbine inlet temperature requires new materials or alloy and / or the usage of efficient means and methods of turbine blades cooling to maintain the blades below thermal failure condition during operation .Modern blades use film cooling to protect the blades outer surface from hot gases . Film cooling is a technique used extensively in turbo machinery. In such situation , coolant air is taken from the compressor and injected through single or multiple rows of holes into the high temperature boundary layer on the blade surface. Film cooling primarily depends on the coolant-to-mainstream mass ratio or can be related to the blowing ratio which can be defined as the ratio of mass flow rate of coolant air to the hot mean stream. In atypical gas turbine blade, the range of the blowing ratios are of about approximately between 0.5 and 2.0.The experiments on a real gas turbine are demanding and it is extremely difficult to obtain results under real engine conditions. Therefore, with the exception of few, all researchers conducted their tests on a flat surface [2].

Hong–wook lee et al [3], concluded that the shaped holes with simple angle injection do not provide substantial improvement in film cooling performance compared to round holes, while shaped holes with compound angle injection exhibit improved film cooling effectiveness up to 55% in comparison with round hole data at high blowing ratios. **Bunker** [4], show that the holes embedded in the trench provided higher film effectiveness distributions than the ones on the plane surface. However, he provided only film effectiveness distributions and also the hole had a compound angle (radial injection) in the lateral direction. Also **Lu et al** [5], showed that the film cooling holes provide higher film effectiveness when embedded in a trench. The heat transfer coefficient enhancement due to the embedding was not significantly higher compared to the typical unimpeded cylindrical hole. The overall heat flux ratio comparing film cooling with embedded holes to unimpeded holes shows that the full trench and downstream trench spacing after the hole exit produce the highest heat flux reduction. **Assim H. Yousif**[6], show that the film cooling performance, film cooling effectiveness and heat transfer coefficient, are enhanced when using two rows of staggered holes with opposite orientation angles**.** More enhancements are obtained when the forward row embedded in rectangular trench as reported by **Mowafak**[12].

At present the film cooling performance, film cooling effectiveness and heat transfer coefficient, are investigated experimentally for two rows of staggered holes with opposite orientated angles, the forward row embedded in arc trench. The aim of present

investigation is to use arc trench instead of rectangular trench to minimize the bad effect of using rectangular trench on the mechanical properties of the gas turbine materials.

Experimental methodology:

A schematic diagram and photograph of the test rig are shown in Figure (1).The mainstream air supply is the ambient air drawn by a blower (1). Manual open gate is used to control the flowing air speed in the test section. The blower exit area having rectangular shape with dimensions of (6.3x13.1) cm. The blower is supplied with bend having the same dimensions of the blower exist and then connected to a diffuser having rectangular cross-section area of inlet and outlet dimensions as (6.3x13.1) cm and (35x50) cm respectively and length of (82) cm. Air flowing through the diffuse occupied with splitter plates into a constant area rectangular settling chamber of cross-section area (35x50) cm and length of 70 cm. The settling chamber after modification contains four grid screens and one row of honeycomb with dimension as (35x50 x20) located behind the electrical heaters to ensure adequate mixing of hot air and uniform temperature distribution throughout the test section.

The warm air routed through a convergent-divergent contraction having a rectangular cross-section area from (35x50) cm to (5x10) cm and length of 70 cm. In order to allow the air to reach the desired temperature, the air is initially routed out away from the test section by using a by-bass gate passage. The temperature of the air is continuously monitored at the exit of the gate and when the desired temperature is reached, the gate is fully opened manually and air flow passes into a test section through a rectangular duct area. To minimize heat losses to the surrounding, the settling chamber and the test section duct are insulated completely. The mainstream Reynolds number based on hole diameter (Red) was taken as (4500).

The operating velocity of the warm air in the test section is kept constant at (20 m/s), while the velocity of coolant air runes at three speeds (9.41, 18.83 and 28.245 m/s) through the experimental program.. The test section has 50mm width and 100mm height. The bottom plate of the test section is made of (234x123) mm Plexiglas of 10mm thickness.

A centrifugal air blower (2) of blowing capacity of (22.17) m^3/min was used to supply the coolant air to the plenum. The plenum was located below the test plate. The coolant air enters a plenum then ejected through holes into the test section. The coolant air pressure is measured at the inlet of the test section.

Digital thermometers were used to measure the mainstream and coolant air temperature. Pre-testing showed that all holes had the same flow rate and temperature conditions. Finally the flow from the coolant holes and the mainstream combine in the test section.

Test model Geometry:

The test model is made from Plexiglas plate containing two rows of staggered holes with opposite orientation angles; the downstream row holes embedded in arc trench. The orientation angles (γ) is defined as the hole orientation toward the cross-flow in the mainstream and the inclination angle(θ)is defined as the angle between the centerline of the hole and the surface of the test wall. Figure (2) shows the rows arrangements. For the downstream row holes, the orientation angles and the inclination

angle are fixed at (ϒ= 0°) and (θ=30°) respectively, while at the upstream row (ϒ) is fixed at (180°) and the inclination angle of upstream holes row ($\theta_{us)}$ are (θ_{us}= 30º). The test surface made from Plexiglas of low thermal conductivity, low lateral conduction, and low thermal diffusivity.

The arrangement of holes geometry were taken as, the hole diameter (D=4mm), the longitudinal distance between the rows (X) is four time (D)i.e. ($\frac{X}{D} = 4$), and the span distance between each neighboring holes (y) is three time (D)i.e. ($\frac{X}{D} = 4$).

Trench dimensions are: depth (0.75D), width (3D), and arc radius (3D).

Instrumentations:

The temperature of warm mainstream air and coolant air were measured by digital thermometer with using thermocouples type-k. A 14mm diameter orifice plate meter is used to measure the coolant air flow rate. A standard ellipsoidal nosed Pitot- static tube with curved junction (N.P.L Standard) is used to measure main stream warm air velocity. The surface temperature of test plate was measured using a single test transient IR thermograph technique by using infrared camera type Fluke Ti32 to precisely record temperature variations. The IR system is greatly affected by both backgrounds temperature and local emissivity. The test surface is sprayed with mat black color to increase the emissivity like a perfect black body. The temperature measurement taken is not accurately recorded unless the IR system is calibrated.

The IR images taken for the test surfaces at each test are stored in the SD memory of IR camera. These images are transferred from SD memory to PC memory. Then the middle region of the test surface area is then selected to eliminate the effect of the test section wall with using camera software facilities. IR images, which exhibit the temperatures distribution as colors code, is converted to corresponding temperature digit values by using Smart View Software and then saved as output data in Excel sheet.

The IR images for models surfaces at each investigated test was captured and stored by thermal camera as image of temperature distributions. These images are transferred to PC. Smart View Software to limit the selected area to avoid the effect of the test section walls .The IR images converted to corresponding temperature digital values and then saved as data in Excel sheet.

Thermal Properties Evaluations:

Thermal quantity of film cooling effectiveness (η) and the heat transfer coefficient (h) can be calculated by using a semi-infinite solid assumption. The test plate is initially at a uniform temperature (*Ti)* at time, t = 0. At time t>0, the flat plate is suddenly exposed to a stream of hot air of temperature (*Tm),* Figure (3) represent the model domain.

The warm stream of air provides a heat flux to the surface of the flat plate and convective heat transfer phenomenon occurs. Balancing thermal energy in the surface of the test plate and conducted only in X-direction yields the following equations:

$$\frac{\partial^2 T}{\partial x^2} = \frac{1}{\alpha}\frac{\partial T}{\partial t} \qquad \ldots (1)$$

Two boundary conditions are needed.

Initial condition to solve this partial differential equation is such as:

At t=0, $T=T_i$

The first boundary condition is at the wall surface,

At, x=0 $-k\frac{\partial T}{\partial x} = h(T_m - T(0,t))$ and t ≥ 0.

The main assumption applied to analyze the transient conduction is the semi-infinite approximation. Therefore, the semi-infinite solid assumptions give an additional boundary condition,

At x = ∞ , $T=T_i$ and t ≥ 0.

The semi-infinite solid assumptions are valid for the present models for two reasons. The test duration is small, usually less than 60 seconds. Secondly, the hot air flowing over the test surface made from adiabatic Plexiglas. The solution of equation 1 is given by [7] as the follow:

$$\frac{T_w - T_i}{T_m - T_i} = 1 - \exp\left[\frac{h^2\alpha t}{k^2}\right] erfc\left[\frac{h\sqrt{\alpha t}}{k}\right] \quad \ldots (2)$$

Where (T_w) is the wall temperature being measured with IR camera. The initial temperature (T_i) of the test surface and the mainstream temperature (T_m) can be measured before and during test respectively. The properties of test surface (k and α) are also known. For infrared technique, t is the time when the IR image was taken after the test was initiated. Therefore, the heat transfer coefficient (h) can be determined.

In film cooling situations, where the coolant air is being injected from the bottom of the plate surface the mainstream in equation (2) must be replaced by a film temperature (T_f), the following equation as given by Ref [8] can be used to estimate(T_f).

$$\frac{T_w - T_i}{T_f - T_i} = 1 - exp\left[\frac{h^2\alpha t}{k^2}\right] erfc\left[\frac{h\sqrt{\alpha t}}{k}\right] \quad \ldots (3)$$

In which (T_f) is a mixed temperature between the mainstream and the coolant temperature and is expected to be in the range of (T_m>T_f>T_c). To determine the unknown (T_f), a non-dimensional temperature is defined as the film cooling effectiveness (η):

$$\eta = \frac{T_f - T_m}{T_c - T_m} \quad \ldots (4)$$

Equation (3) has two unknowns, (h and T_f), to solve this equation, two sets of data points required to obtain the unknowns like:

$$\frac{T_{w1} - T_i}{T_f - T_i} = 1 - exp\left[\frac{h^2\alpha t_1}{k^2}\right] erfc\left[\frac{h\sqrt{\alpha t_1}}{k}\right] \quad \ldots (5)$$

$$\frac{T_{w2} - T_i}{T_f - T_i} = 1 - exp\left[\frac{h^2\alpha t_2}{k^2}\right] erfc\left[\frac{h\sqrt{\alpha t_2}}{k}\right] \quad \ldots (6)$$

In this case, a transient infrared thermograph technique will be used to obtain both h&η from a single test as described by Ekkad [9]. Thus, two images with surface temperature distributions are captured at two different times during the transient test.

A net heat flux ratio is the ratio of heat flux to the surface with film cooling to the heat flux without film cooling. This term is used to measure the combined effect of film effectiveness and heat transfer coefficient [10].

$$\frac{q''}{q_o''} = \frac{h}{h_o}\left(1 - \frac{\eta}{\emptyset}\right) \qquad \ldots (7)$$

The values for the overall cooling effectiveness (∅) are ranging between(0.5 and 0.7)according to [11] for the present work (∅) take equal to(0.6).

MATLAB program Software is prepared using a semi-infinite solid assumption presented to solve the above equations (4, 5, 6 and 7). The data used to introduce the film cooling effectiveness and heat transfer coefficient contours from the selected area presented denoted by (A_o).

RESULTS AND DISCUSSIONS:

Contours of film cooling effectiveness and heat transfer coefficient are calculated from, the test surface temperature distribution, and the measurement of the hot mainstream and coolant air temperatures**.** Figures (5 and 6) show the effect of blowing ratio on detailed film effectiveness distributions. Figure (5) presented the distribution of the local heat transfer coefficient (h) andFigure (6) presented the local film cooling effectiveness(η) at three BRs.It appears that the trench provide good performance in the region between any two neighboring holes especially in region near hole exit.According to [12] the downstream wall of the slot may provide an obstruction to the coolant jet and as a result, the coolant jet is spread laterally into the trench and decreases the momentum of the jet and hence reduction in the jet lift-off as well as ejecting out attached to the surface, a parameters that controlled the film cooling performance are blowing ratio and the shape and type of vortex that formed at interaction between the coolant air and hot mainstream.

Figure (7) presents the effect on span wise averaged film effectiveness. This Figures shows clearly that the highest value of the average effectiveness for BR=0.5 was (0.77) at (X/D=0) The spanwise average film effectiveness for present model at hole exit are higher than that of the same model with rectangular trench of same dimension of present arc trench, given by Ref [12], this behavior continue up to (X/D=2),and after that when (X/D=3) the value of (η_{sa}) for rectangular trench become higher than the present model, but this behavior continue up to (X/D=10).

For BR=1.0, the maximum value of (η_{sa}) was at (X/D=0) equal to (0.67). When comparing with results of Ref [12] for rectangular trench, the value of (η_{sa}) for rectangular are higher than that for present model, this behavior continue up to (X/D=2) and after that (from X/D=2 up to X/D=18) the value of (η_{sa}) for present model become higher than that of rectangular model, and at (X/D> 18).

For BR=1.5,the maximum value of (η_{sa}) at (X/D=0) is (0.69). In comparing with rectangular, present values of (h_o) at (X/D=0) is lower than that of rectangular model, at (X/D=1) to (X/D=3) the value of (η_{sa}) for present model become lower, between (X/D=4) to (X/D=12), while when (X/D> 12) the value of (η_{sa}) for present model become higher as shown in figure (7).

The overall average film effectiveness (η_{av}) for the entire selected area Ao(η_{sa}) was calculated from the value of local film effectiveness (η_{sa}) for the entire pixel values included by area (Ao). The overall average film effectiveness (η_{av}) value for the present model is increased by about (0.84%)at BR=0.5 and about (0.43%)at BR=1.0 and decreased by about (0.037%) at BR=1.5 in comparing with that of rectangular trench as shown in figure (8).

The average of local heat transfer coefficient ratio (h/ho), (h) represent the heat transfer coefficient on the plate surface with film cooling and (ho) represent the heat transfer coefficient without film cooling, is presented in figure (9). The value of (h/ho)for present model is higher by (1.918) than that of rectangular model at BR=0.5. At BR1.0 and BR=1.5 the value of (h/ho) for present model are lowest by (0.277) and (0.32) respectively than that of rectangular trench.

The heat load can be presented by combining the heat transfer coefficient ratio (h/ho) and the film cooling effectiveness (η), according to equation (7).Figure (10) shows the effect of the blowing ratio on the overall heat flux ratio (q/q_o) it is clear that from this figure the present model have higher value of (q/q_o) at BR=0.5 than that of rectangular by (0.117), at high blowing ratio BR=1.0 and BR=1.5 the present model show relatively slight lower values of (q/q_o) than that of rectangular trench by (0.059) and (0.025) respectively.

CONCLUSIONS:

For the same holes arrangements the comparison between existing rectangular trench and present arc trenches the film cooling thermal performance for both cases are approximately very close with slight differences according to the values of blowing ratios. The average of local heat transfer coefficient ratio (h/ho) for arc trench was found to be higher than that of rectangular trench at BR=0.5, while at BR1.0 and BR=1.5 the value of (h/ho) was found to be slightly lower than that of rectangular trench. The overall heat flux ratio (q/qo) for arc trench have higher value than that of rectangular trench at BR=0.5, while at higher blowing ratios (BR=1.0 and BR=1.5), (q/qo) had relatively lower values than that of rectangular trench.

REFERENCE:

[1] Sanjay Kumar &Onkar Singh, 2008, "Thermodynamic evaluation of different gas turbine blade cooling techniques", Thermal Issues in Emerging Technologies, ThETA 2, Cairo, Egypt.

[2] A. Azzi and M. Abidat,2001, "film cooling prediction of simple and compound angle injection from one and two staggered rows", Numerical Heat Transfer, Part A, 40: 273± 294. Taylor & Francis.

[3] Hong – Wook Lee , Jung Joon Park , JoonSike Lee,2002, "flow visualization and film cooling effectiveness measurements around shaped holes with compound angle orientations" , International Journal of Heat and Mass Transfer 45 145-156.
[4] Bunker, R.S., 2002, "Film Cooling Effectiveness due to DiscreteHoles within a Transverse Surface Slot," ASME Paper GT-2002-30178.
[5] Lu, Y., Nasir, H., and Ekkad, S.V., 2005, "Film Cooling From aRow of Holes Embedded in Transverse Slots," ASME PaperIGTI2005-68598.
[6] Assim H. Yousif,2012, "Thermal Performance of Film Cooling for Two Staggered Rows of Circular Jet", university of technology.
[7] Nag, P.K., 2007 "Heat and Mass Transfer", second edition, New Delhi, McGraw-Hill.
[8] Holman, J.P., 2008, "Heat Transfer", Ninth Edition, McGraw-Hill Companies,Inc., New York.
[9] Ekkad, S. V., Ou S. and River, R. V., 2004, "A Transient Infrared Thermography Method for Simultaneous Film Cooling Effectiveness and Heat Transfer Coefficient Measurements from a Single test" GT2004-54236, Proceedings of ASME Turbo Expo, Vienna, Austria.
[10] Ekkad, S. V., and Zapata, D., 1997, "Heat Transfer Coefficients Over a Flat Surface with Air and CO2 Injection Through Compound Angle Holes Using a Transient Liquid Crystal Image Method," ASME Journal of Turbomachinery Vol. 119, No. 3, pp. 580-586.
[11] Albert, J.E., Cunha, F. and Bogard, D.G., 2004, "Adiabatic and Overall Effectiveness for a Film Cooling Blade", ASME Paper GT2004-53998.
[12] Muwafaq S.Alwan, 2012, "Experimental and NumericalInvestigation of Film Cooling ThermalPerformance for Staggered Rows of Circular Jet", PH.D thesis, University of Technology.

Nomenclatures:

BR Blowing ratio
D Film hole diameter
h Heat transfer coefficient with coolant injection
h_oHeat transfer coefficient without coolant injection.
kThermal conductivity of test surface.
q Heat flux with coolant injection.
q_oHeat flux without coolant injection.
T_cCoolant temperature.
T_i Initial temperature.
T_m Hot mainstream temperature.
T_wWall temperature.
*Uc*Coolant velocity.
Um Hot mainstream velocity.
X parallel dimension to the surface.
x perpendicular dimension to the surface.

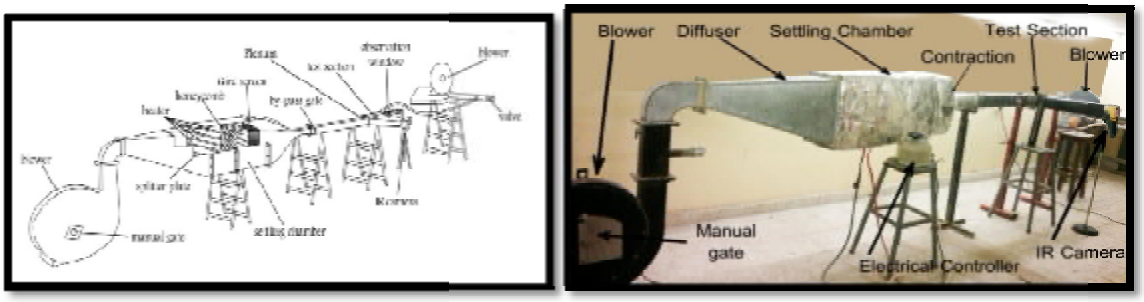

Figure (1) Schematic and photography of the experimental rig.

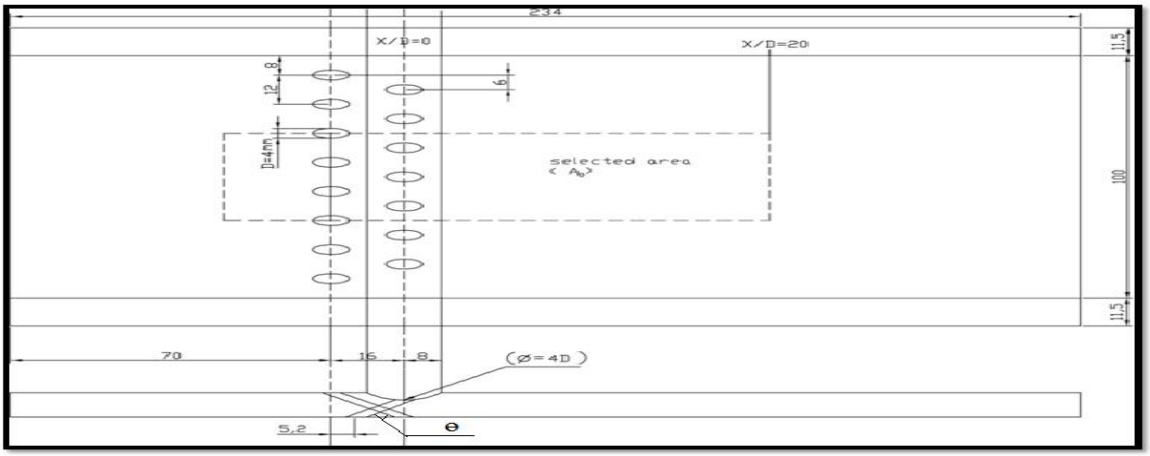

Figure (2) a top and side view with middle selected area of the test section (A_o)
(a)Forward injection$\theta = 30^{\circ}\&\gamma = 0^{\circ}$(b)backward injection$\theta = 30^{\circ}\&\gamma = 180$

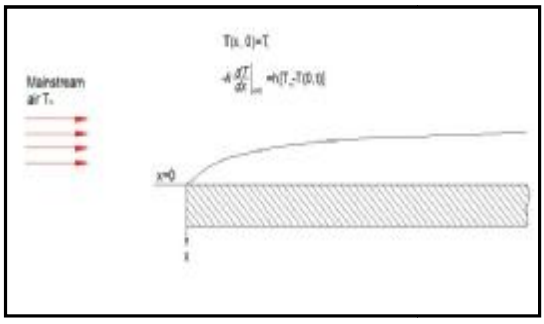

Figure (3) Flow over flat plate

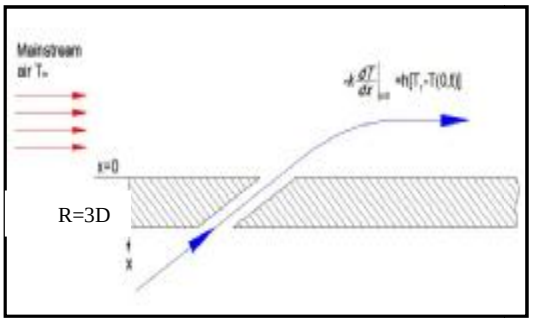

Figure (4) Film cooling over flat plate

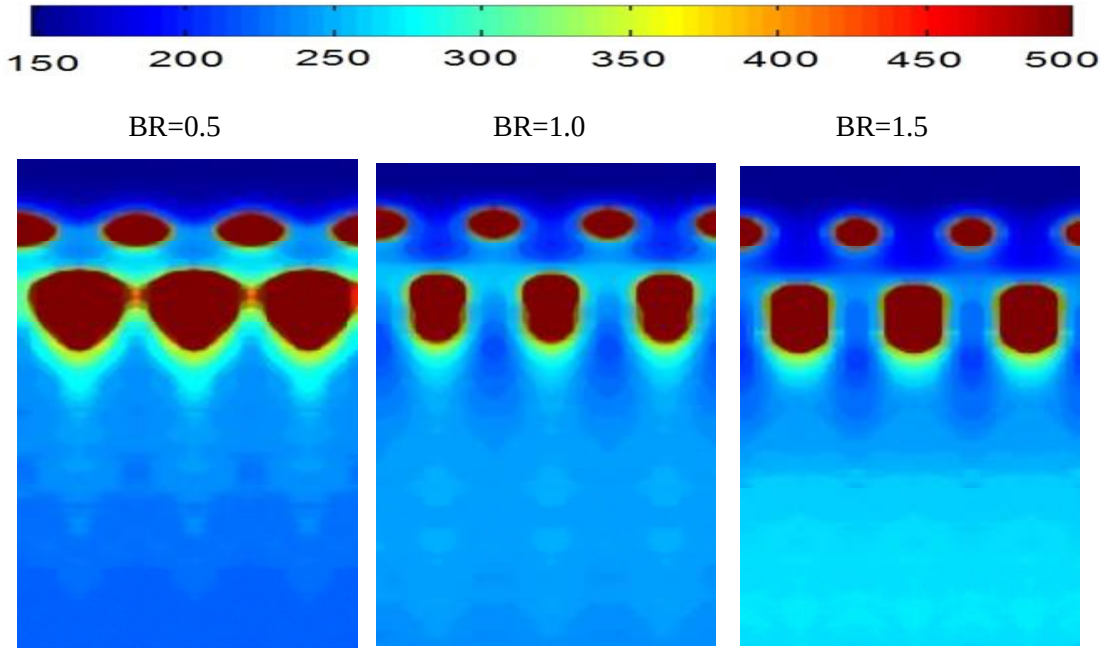

Figure (5) Contours of heat transfer coefficient

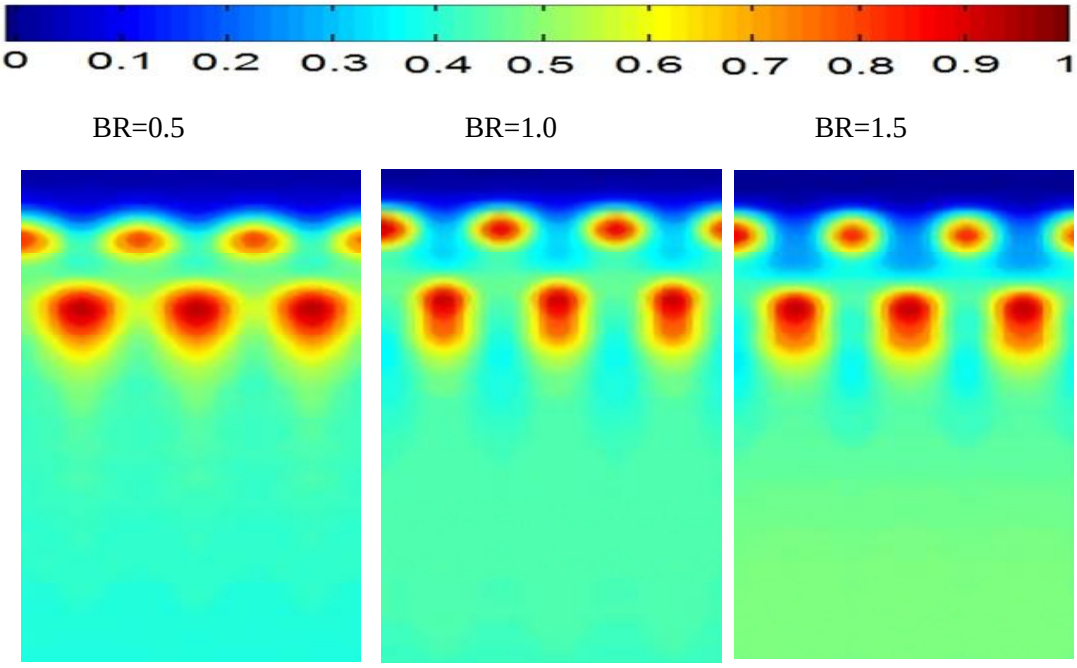

Figure (6) Contours of film cooling effectiveness.

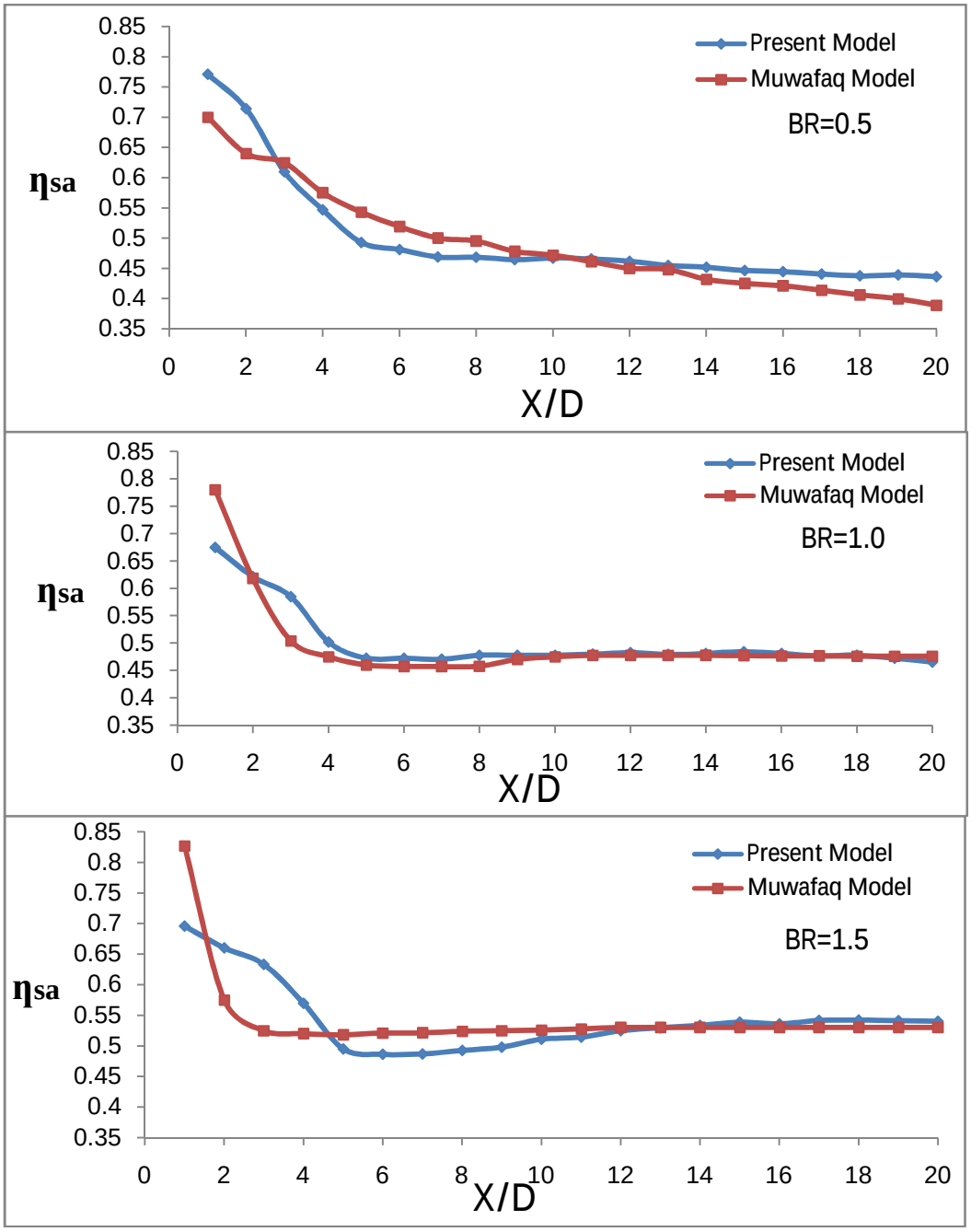

Figure (7) The comparison of the spanwise average film cooling effectiveness with Ref (12) at different BRs.

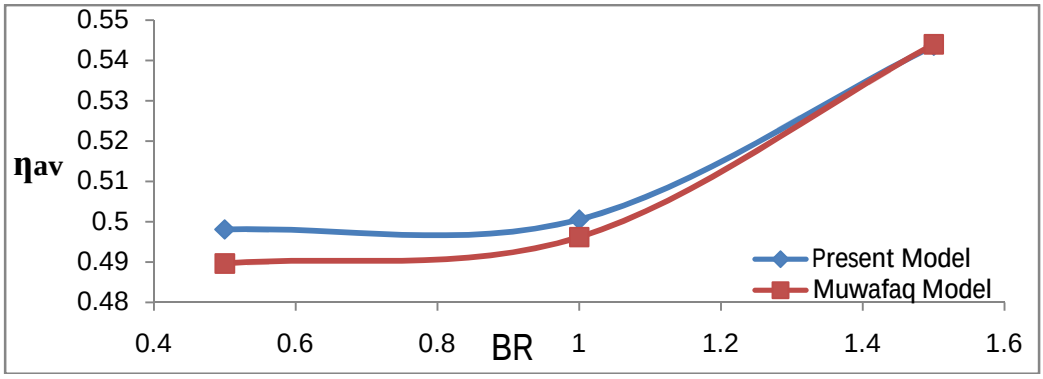

Figure (8) Effect of blowing ratio on averaged film cooling effectiveness.

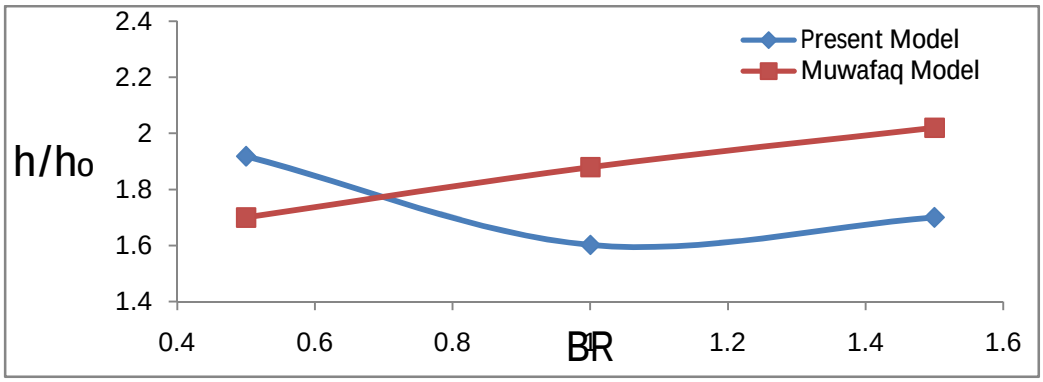

Figure (9) Effect of blowing ratio on averaged heat transfer coefficient ratio.

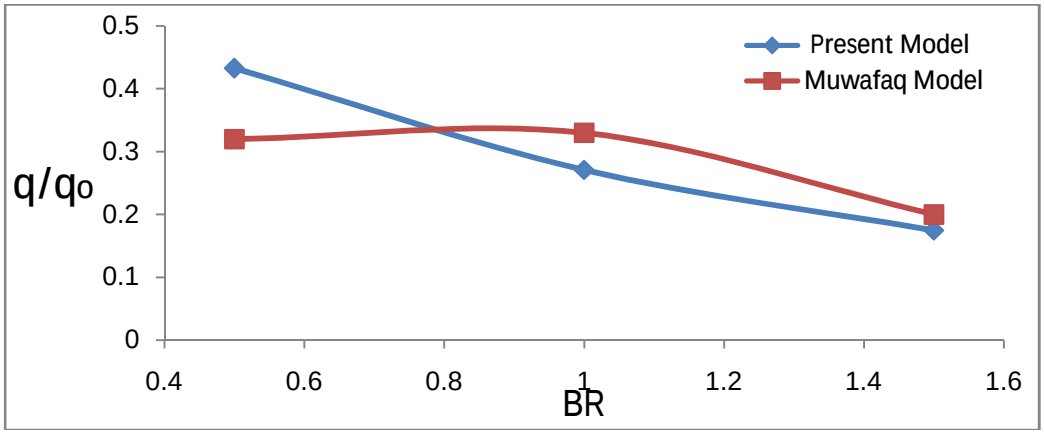

Figure (10) Effect of blowing ratio on overall heat flux ratio.